DOI: 10.1002/ejic.200800158

Designed Synthesis of Families of Misfit-Layered Compounds

Qiyin Lin,[a] Colby L. Heideman,[b] Ngoc Nguyen,[b] Paul Zschack,[c] Catalin Chiritescu,[d] David G. Cahill,[d] and David C. Johnson*[b]

Keywords: Incommensurate structure / Synthesis design / Nanostructure / Crystal engineering / Layered compounds

The synthesis of several new families of misfit-layered compounds is demonstrated. These compounds are crystalline along the *c*-axis and in the *ab*-plane, but show very short coherence lengths between *ab*-planes. This disorder leads to ultra-low and tunable thermal conductivity. Annealing isostructural samples under a chalcogen vapour until equilibrium is reached results in reproducible Seebeck and resistivity values.

Introduction

Recently, Cahill and collaborators reported an exceptionally low thermal conductivity ($0.05\ \mathrm{W\,m^{-1}\,K^{-1}}$) for turbostratically disordered tungsten diselenide.[1] This material had an unusual structure. It was ordered in the *c*-direction with the domain size approximately equal to the thickness of the film (typically 50–100 nm). It also showed well-ordered and crystallized *ab*-planes with typical coherence lengths of 6–7 nm, but had rotational disorder between the planes that resulted in a very short coherence length of 1–2 nm in any other crystallographic direction. When the in-plane and *c*-axis order were destroyed by ion implantation, the thermal conductivity increased, approaching the expected theoretical minimum for this material. This suggests that this unusual disordered structure was a key factor in the low thermal conductivity and that other materials with this disorder might also have extremely low thermal conductivities.

One class of materials where this unusual balance of order and disorder might be a natural consequence of the crystal structure is that of the misfit-layered compounds initially reported by Diaz and co-authors in 1985.[2] These compounds consist of intergrowths of distorted rock salt layers with dichalcogenide layers as shown in Figure 1. These compounds have the general chemical formula $[(MX)_{1+x}]_m(TX_2)_n$ where X = S and Se, M = Sn, Pb, Sb, Bi, and rare earth metals. The TX_2 layer is traditionally composed of T = Ti, V, Cr, Nb and Ta.[3,4] The "misfit" in this structure is given by x, which ranges from 0.07 to 0.28 in compounds reported to date.[5,6] The distortion in the rock salt results from the coordination of M by X from the TX_2 layer.[7] The values m and n represent the number of rock salt bilayers and the number of X-T-X planes in the unit cell, respectively. While an infinite family of compounds with different m and n values should in theory exist, typically only one or two members of any family of compounds has been prepared with $m = 1$ and $n = 1$ or 2 accounting for the vast majority of reported compounds.[3,4] Of the ca. 80 known misfit-layered compounds prepared by direct combination of the elements, only 9 are selenides.[8–13] These compounds are structurally ordered, with several single-crystal structures reported. Charge transfer is generally accepted as the stabilizing mechanism for the misfit struc-

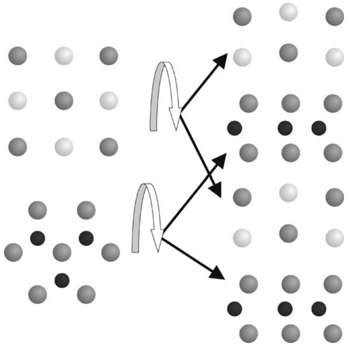

Figure 1. Typical structure projected along [001] for the binary components (left) and along [100] for the superlattice structure of $[(MX)_{1+x}]_1(TX_2)_1$ showing a generic stacking scheme observed in these materials (right). The slight buckling in the MX layer results from the coordination of the M atoms by the chalcogen atom from the TX_2 layer. M, T, and X atoms are represented by light, dark, and intermediate shade, respectively.

---

[a] Department of Physics, University of Oregon,
1274 University of Oregon, Eugene, OR 97403, USA
[b] Department of Chemistry, University of Oregon,
1253 University of Oregon, Eugene, OR 97403, USA
Fax: +1-541-346-0487
E-mail: davej@uoregon.edu
[c] Advanced Photon Source, Argonne National Laboratory,
9700 S. Cass Avenue, Argonne, IL 60439, USA
[d] Department of Materials Science and Engineering and Materials Research Laboratory, The University of Illinois,
104 S. Goodwin Ave., Urbana, IL 61801, USA

Supporting information for this article is available on the WWW under http://www.eurjic.org or from the author.

ture over a physical mixture of the components.[14] While there are many reports on the electrical properties of these materials, there is only one report on the lattice thermal conductivity of these materials, with a value of 0.8 $\mathrm{W\,m^{-1}\,K^{-1}}$ reported for $[(YbS)_{1.24}]_1(NbS_2)_1$.[15]

Results and Discussion

This report presents the successful preparation of over 60 new misfit-layered selenides in five selenide families by a synthetic approach that provides access to many members of each family. The new misfit-layered compounds $[(MX)_{1+x}]_m(TX_2)_n$ were self-assembled from designed precursors prepared by sequentially depositing m bilayers containing M and X in a 1:1 atomic ratio followed by n bilayers containing T and X in a 1:2 ratio. In each bilayer, the ratio of the layer thicknesses was adjusted to obtain the composition corresponding to the stoichiometry of the desired component compound, and the absolute thickness of each bilayer was adjusted to provide the number of atoms required to form an MX rock salt bilayer or X-T-X dichalcogenide trilayer. Figure 2 shows the evolution of a diffraction pattern as a function of annealing temperature from a film designed to form $[(BiSe)_{1.10}]_1(NbSe_2)_1$. The as-deposited diffraction scan contains no low-angle diffraction maxima corresponding to the as-deposited layers, suggesting significant interdiffusion. Only weak broad maxima occur at higher angles. As a function of annealing temperature and time, we observe the growth of intense (00*l*) diffraction maxima as the film self-assembles into the targeted, crystallographically textured misfit compound. The texture in the samples was confirmed by rocking curve scans, which show that the alignment increases with annealing temperature and time with a rocking curve width that narrows from 11.3° as deposited to 2.7° after annealing at 350° for 2 h.

Figure 3 shows the diffraction patterns of 4 $[(PbSe)_{0.99}]_m(WSe_2)_n$ compounds prepared by varying m and n. The misfit of 0.99 was calculated from the in-plane unit cell dimensions of each component.[3,4] In this particular family of compounds, we have prepared the first 25 compounds, where $1 \leq m,n \leq 5$. This permits us to examine the regular change in the lattice parameter as n and m are varied. Figure 4 contains graphs of the regular changes in lattice parameter observed as n and m are varied in the five systems investigated to date, demonstrating the ability to prepare specific compounds in several classes of materials. For the $[(PbSe)_{0.99}]_m(WSe_2)_n$ family, a regular change of 0.654 nm is observed where m is kept constant and n is incremented by 1. A value of 0.614 nm is observed when increasing m.

The extent of structural coherence and the grain sizes of the crystalline domains vary as a function of annealing time and temperature. Typically, temperatures around 350 °C are sufficient to self-assemble the targeted compounds. The compounds are stable for extended annealing times at temperatures up to at least 550 °C in sealed ampoules to prevent loss of selenium. At the optimal annealing temperature, 00*l* diffraction maxima are observed to beyond 2θ =

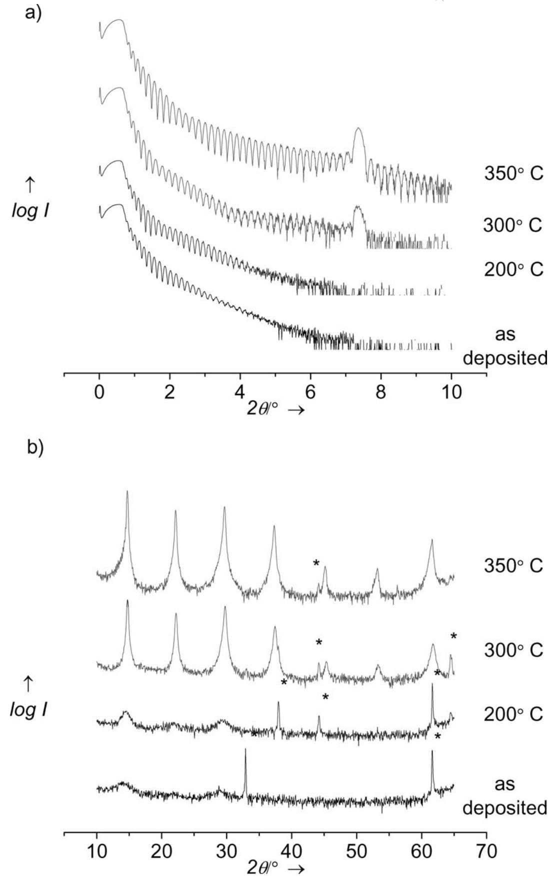

Figure 2. Evolution of (a) the low-angle reflectivity data from 2θ = 0° to 10° and (b) the high-angle diffraction data as a function of annealing temperature of a precursor film designed to evolve into $[(BiSe)_{1.10}]_1(NbSe_2)_1$. The low-angle data shows significant smoothing of the film as kiessig fringes extend out to higher angles with annealing. The growth of the superlattice is evident in the high-angle pattern, with the first 8 00*l* diffraction lines emerging as a function of annealing temperature and time. (*) indicates substrate or stage peaks which vary based on the mounting of the sample in the goniometer.

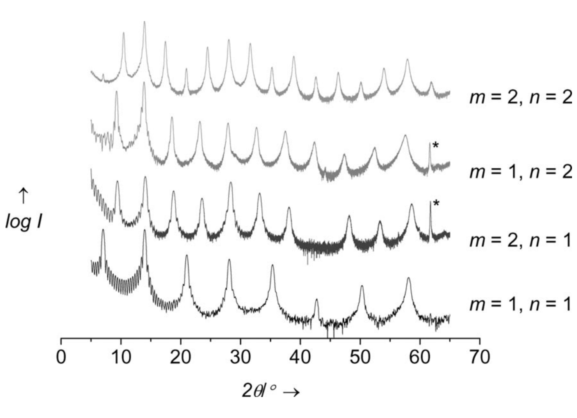

Figure 3. Diffraction patterns of four $[(PbSe)_{0.99}]_m(WSe_2)_n$ compounds after annealing at 400 °C for 1 h. The unit cells calculated for each material show a regular increase in the c-axis of the unit cell. (*) indicates substrate peaks.

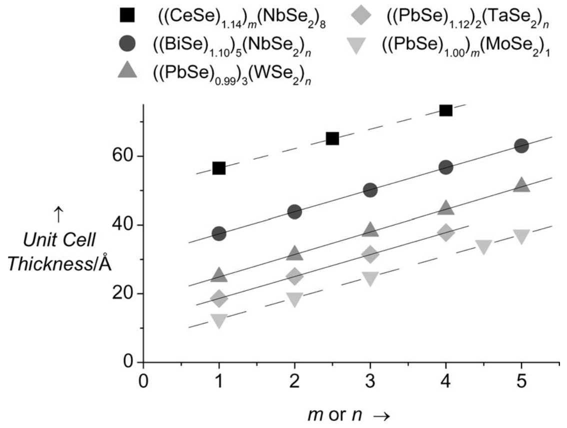

Figure 4. Plot of the size of the unit cell along the *c*-axis as a function of the number of repeat layers for five different systems. Solid lines correspond to increasing the number of dichalcogenide layers and dashed lines to increasing the number of rock-salt layers, in each case the thickness of the other component being kept constant.

74° resulting from the structural order of the interwoven layers along this direction. In the *ab*-plane, the expected *hk*0 diffraction maxima are observed for the structures of each of the components. In $[(PbSe)_{1.00}]_m(MoSe_2)_n$ for example, the *a*-lattice parameters are found to be 0.6163 ± .0003 nm for PbSe and 0.3310 ± 0.0009 nm for $MoSe_2$. These values compare with 0.6121 nm and 0.3289 nm, respectively, observed in the bulk binary compounds.[16–22] Interestingly, this unit cell leads to an approximately rational 1:1 stoichiometry between the two constituent components. This ratio is significantly smaller than has previously been observed in this class of compounds. The in-plane coherence length within the rock salt is significantly larger than within the $MoSe_2$, at roughly 13 nm for PbSe and 6 nm for $MoSe_2$. Area diffraction patterns show that the film coherence length between layers can be controlled by changing the thickness of the rock salt component as well as annealing temperature and time. In the area diffraction pattern collected for $[(PbSe)_{1.00}]_2(MoSe_2)_1$, satellite reflections corresponding to the superlattice structure are observed between brighter spots resulting from the overlap of *hkl* reflections for lead selenide. These satellite peaks can be indexed with very good agreement to lattice parameters determined from in-plane and cross-plane diffraction data. Area diffraction data collected for $[(PbSe)_{1.00}]_1(MoSe_2)_2$ do not contain the satellite reflections corresponding to the superlattice structure. In each case, the peak widths of the *hkl* diffraction spots are much broader than *hk*0 or 00*l* spots, indicating a much shorter coherence length due to plane-to-plane disorder.

The compounds reported here are unique relative to the misfit compounds reported to date, both in the extent of the misfit and in the ability to prepare compounds where little charge transfer between the components would be anticipated. The physical properties of these materials are just beginning to be investigated. We have observed metallic behavior in systems containing $NbSe_2$ as the dichalcogenide, in agreement with prior work done on sulfides.[23,24] The compounds of the form $[(PbSe)_{0.99}]_m(WSe_2)_n$ or $[(PbSe)_{1.00}]_m(MoSe_2)_n$ are semiconducting. The thermal conductivity of PbSe layered with WSe_2 and $MoSe_2$ have shown thermal conductivities as low as $0.06\ W\,m^{-1}\,K^{-1}$. This is up to an order of magnitude lower than the only other report on the lattice thermal conductivity of a misfit layered compound.[15] The electrical properties of samples after annealing under open N_2 tend to vary significantly from sample to sample due to small changes in composition and varying defect levels. We have discovered that annealing the samples in an overpressure of selenium, produced by a large excess of one of the binary components as a vapor source in the sealed ampoule, equilibrates the carrier concentrations and defect levels. Figure 5 shows the effect of annealing three $[(PbSe)_{0.99}]_1(WSe_2)_1$ films under open N_2 followed by annealing in a controlled vapor pressure of chalcogen for different lengths of time.

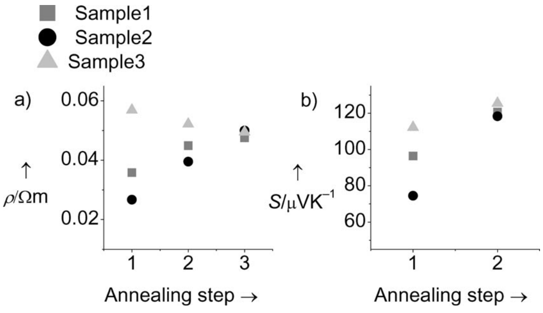

Figure 5. Electrical properties of 3 identical samples of $[(PbSe)_{0.99}]_1(WSe_2)_1$ annealed (1) under open N_2 at 400 °C for 1 h; (2) in a sealed environment with an Se overpressure at 400 °C for 1 h; (3) in a sealed Se environment at 400 °C for 2 h.

Conclusions

By using modulated elemental precursors, we have demonstrated that entire families of misfit-layered compounds can be synthesized with far greater variability in structure and properties than has been previously demonstrated. By using this synthetic technique, the balance between order and disorder can be tuned. While our initial efforts have focused on the synthesis and structural characterization, we believe the ability to prepare many compounds in a particular family and to vary the carrier concentration through annealing in a controlled chalcogen environment will enable systematic studies on the variation of physical properties as a function of *n* and *m*.

Experimental Section

Compounds were synthesized in a custom-built ultra-high-vacuum deposition system, described elsewhere.[25] Samples were synthesized under 10^{-7} Torr. Metals W, Nb, Mo, Ce, Bi, and Pb were deposited from an electron beam gun at a rate of 0.2 or 0.4 Å/s, and Se was deposited from an effusion cell at a rate of 0.5 Å/s. A computer-controlled quartz-crystal monitoring system was used to control layer thicknesses. Samples were deposited on (100) silicon wafers at ambient temperature with a total thickness in the range of 20–80 nm. Deposition parameters were determined to yield the appropriate stoichiometry required for a single rock-salt layer or transition-metal dichalcogenide trilayer. The two subsystems were thus brought together as a precursor to form these homologous compounds composed of the two subsystems. Assembly of the desired structures typically occurs between 350 and 400 °C after annealing for 1 h under nitrogen. Further annealing steps were conducted in a sealed quartz ampoule where bulk powder of one of the components was used to supply a controlled chalcogen vapor pressure. The crystalline quality, orientation, and thickness of the films were evaluated by high-resolution X-ray diffraction and reflectivity using a Bruker D8 Discover diffractometer with Cu-$K_{\alpha 1}$ radiation. The *ab*-plane and 2D X-ray diffraction patterns were collected by using synchrotron radiation at the Advanced Photon Source (APS) (33BM and 33ID) at the Argonne National Laboratory. Electrical measurements along the *ab*-planes of the thin films of $[(PbSe)_{0.99}]_m(WSe_2)_n$ were carried out by a DC four-probe method in the van der Pauw configuration. The Seebeck coefficient (*S*) of the films was measured by a conventional steady-state method. Cross-plane thermal conductivity measurements were conducted using time-domain thermoreflectance.

Supporting Information (see footnote on the first page of this article): Further data pertaining to the in-plane and off-axis structure.

Acknowledgments

The use of the APS was supported by the U. S. Department of Energy, Office of Science, Office of Basic Energy Sciences, under contract no. DE-AC02-06CH11357 This work was supported by the National Science Foundation (DGE-0549503) and the Office of Naval Research (N0014-07-1-0358).

---

[1] C. Chiritescu, D. G. Cahill, N. Nguyen, D. Johnson, A. Bodapati, P. Keblinski, P. Zschack, *Science* **2007**, *315*, 351–353.
[2] L. Otero-Diaz, J. D. FitzGerald, T. B. Williams, B. G. Hyde, *Acta Crystallogr., Sect. B: Struct. Sci.* **1985**, *41*, 405–410.
[3] G. A. Wiegers, A. Meerschaut, *Mater. Sci. Forum* **1992**, *100–101*, 101–172.
[4] G. A. Wiegers, *Prog. Solid State Chem.* **1996**, *24*, 1–139.
[5] Y. Gotoh, M. Onoda, J. Akimoto, M. Goto, Y. Oosawa, *Jpn. J. Appl. Phys., Part 1* **1992**, *31*, 3946–3950.
[6] A. Lafond, C. Deudon, A. Meerschaut, A. Sulpice, *Eur. J. Solid State Inorg. Chem.* **1994**, *31*, 967–978.
[7] S. Van Smaalen, A. Meetsma, G. A. Wiegers, J. L. De Boer, *Acta Crystallogr., Sect. B: Struct. Sci.* **1991**, *47*, 314–325.
[8] V. Petricek, I. Cisarova, J. L. De Boer, W. Zhou, A. Meetsma, G. A. Wiegers, S. Van Smaalen, *Acta Crystallogr., Sect. B: Struct. Sci.* **1993**, *49*, 258–266.
[9] R. Roesky, A. Meerschaut, J. Rouxel, J. Chen, *Z. Anorg. Allg. Chem.* **1993**, *619*, 117–122.
[10] Y. Oosawa, Y. Gotoh, J. Akimoto, T. Tsunoda, M. Sohma, M. Onoda, *Jpn. J. Appl. Phys., Part 2* **1992**, *31*, L1096–L1099.
[11] Y. Ren, J. Baas, A. Meetsma, J. L. de Boer, G. A. Wiegers, *Acta Crystallogr., Sect. B: Struct. Sci.* **1996**, *52*, 398–405.
[12] M. H. Van Maaren, *Phys. Lett. A* **1972**, *40*, 353–354.
[13] W. Y. Zhou, A. Meetsma, J. L. De Boer, G. A. Wiegers, *Mater. Res. Bull.* **1992**, *27*, 563–572.
[14] A. Meerschaut, Y. Moelo, L. Cario, A. Lafond, C. Deudon, *Mol. Cryst. Liq. Cryst.* **2000**, *341*, 1–8.
[15] Y. Miyazaki, H. Ogawa, T. Kajitani, *Jpn. J. Appl. Phys., Part 2* **2004**, *43*, 1202–1204.
[16] H. E. Swanson, N. T. Gilfrich, G. M. Ugrinic, *National Bureau of Standards Circular (U. S.)* **1955**, *5*, 75.
[17] Y. Noda, S. Ohba, S. Sato, Y. Saito, *Acta Crystallogr., Sect. B: Struct. Sci.* **1983**, *39*, 312–317.
[18] Y. Noda, K. Masumoto, S. Oba, Y. Saito, K. Toriumi, Y. Iwata, I. Shibuya, *Acta Crystallogr., Sect. C: Cryst. Struct. Commun.* **1987**, *43*, 1443–1445.
[19] C. Auriel, R. Roesky, A. Meerschaut, J. Rouxel, *Mater. Res. Bull.* **1993**, *28*, 247–254.
[20] K. D. Bronsema, J. L. De Boer, F. Jellinek, *Z. Anorg. Allg. Chem.* **1986**, *540–541*, 15–17.
[21] L. C. Towle, V. Oberbeck, B. E. Brown, R. E. Stajdohar, *Science* **1966**, *154*, 895–896.
[22] F. Cech, M. Rieder, S. Vrana, *Neues Jahrb. Mineral., Monatsh.* **1973**, 433–442.
[23] G. A. Wiegers, A. Meetsma, R. J. Haange, J. L. De Boer, *Solid State Ionics* **1989**, *32–33*, 183–191.
[24] G. A. Wiegers, A. Meetsma, R. J. Haange, J. L. De Boer, *J. Solid State Chem.* **1990**, *89*, 328–339.
[25] L. Fister, X.-M. Li, J. McConnell, T. Novet, D. C. Johnson, *J. Vac. Sci. Technol.* **1993**, *11*, 3014–3019.

Received: February 12, 2008